NMR of Short-Chain Hydrocarbons in Nematic and Smectic A Liquid Crystals

ARTICLE *in* THE JOURNAL OF PHYSICAL CHEMISTRY A · AUGUST 2013

Impact Factor: 2.69 · DOI: 10.1021/jp404315t · Source: PubMed

THE JOURNAL OF PHYSICAL CHEMISTRY A

Article

pubs.acs.org/JPCA

NMR of Short-Chain Hydrocarbons in Nematic and Smectic A Liquid Crystals

Adrian C. J. Weber[§]

Chemistry Department, Brandon University, 270 18th Street, Brandon, MB, R7A 6A9 Canada

Ronald Y. Dong[†]

Physics Department, University of British Columbia, 6224 Agricultural Road, Vancouver, British Columbia, V6T 1Z1 Canada

W. Leo Meerts[‡]

Institute for Molecules and Materials, Radboud University, Heyendaalseweg 135, NL-6525 AJ Nijmegen, The Netherlands, and Laser Centre, Vrije Universiteit, De Boelelaan 1081, 1081 HV Amsterdam, The Netherlands

Xuan Yang and E. Elliott Burnell*

Chemistry Department, University of British Columbia, 2036 Main Mall, Vancouver, British Columbia, V6T 1Z1 Canada

Supporting Information

ABSTRACT: The proton NMR spectra of ethane, propane, and *n*-butane codissolved and orientationally ordered in two liquid-crystal solvents that exhibit both nematic (N) and smectic A (SmA) phases (one of which also has a reentrant nematic (RN) phase) are analyzed using CMA-ES (covariance-matrix adaptation evolution strategy). To deal with problems arising from the broad liquid-crystal background signal, a smoothed experimental spectrum is fitted to a smoothed calculated spectrum. The ethane and propane dipolar couplings and anisotropic energy parameters scale with each other, and the *n*-butane couplings are assumed to behave likewise. This restriction on the relative values of the *n*-butane energy parameters facilitates a fit to the temperature dependence of the *n*-butane dipolar couplings, in which the six *n*-butane energy parameters (three for trans and three for gauche), the isotropic trans−gauche energy difference E_{tg}, and its temperature coefficient E'_{tg}, and the methyl CCH angle decrease are obtained. Unlike earlier studies, the fit does not employ a model for the anisotropic intermolecular potential. The nematic potential in the SmA phase of the liquid-crystal mixture 6OCB/8OCB is estimated by interpolated values obtained from the ethane spectra for the N and RN regions. Analysis of results for the SmA phase involves adding a nematic−smectic coupling prefactor and a smectic prefactor. Spectra obtained in the liquid-crystal 8OCB are calculated with no adjustable parameters, scaling the potentials using the ethane values, and the agreement between experiment and calculation is outstanding. Conformer populations are affected by the environment, and the isotropic solute−solvent interactions result in increased gauche populations, whereas anisotropic interactions increase the trans probability. The trans probability in the SmA phase is slightly lower than expected from the nematic results.

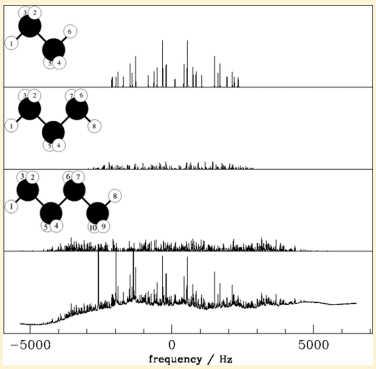

1. INTRODUCTION

Oriented molecular fluids (liquid crystals) play a vital role in a wide variety of systems (e.g., computer and TV displays, biomembranes, and industrial applications) that affect our everyday lives. Liquid crystals form a fascinating array of macroscopic structures and are characterized predominantly by the long-range orientational (and in some cases positional) order of the component molecules.

Liquid crystals in general consist of flexible molecules and, in particular, usually contain flexible hydrocarbon chains. The flexibility arises from the possibility that each saturated C−C link can be in a trans or in a gauche conformation. The populations of various conformations is an important property that is difficult to measure precisely, and the effect of the orientational (and possibly positional) ordering on conformer populations poses a particularly interesting question.

NMR (nuclear magnetic resonance) of orientationally ordered systems can yield a vast amount of information. In

Received: May 1, 2013
Revised: July 23, 2013
Published: August 20, 2013

general the liquid-crystal molecules contain many spins and give rise to a broad spectrum of many unresolved transitions. On the other hand, the NMR spectra of solutes that are orientationally (and positionally) ordered by the anisotropic phase and that do not contain too many coupled nuclear spins give rise to spectra that are in general analyzable, yielding chemical shifts, indirect spin−spin couplings, and direct dipolar couplings. Analysis of these NMR spectra yields very accurate solution-state geometries, anisotropies of chemical shifts and indirect spin−spin couplings, as well as average degrees of solute orientational order.

As hydrocarbon chains are an important ingredient to liquid crystals in general, the understanding of the simpler hydrocarbon solutes (for example *n*-butane) is of particular interest. Several deuteron NMR investigations of hydrocarbons as solutes in nematic liquid crystals have been reported, and models for orientational order have been used in the interpretation of the results.[1,2] Indirect spin−spin *J* couplings have been obtained from analysis of high-resolution isotropic-solution-state NMR spectra of *n*-butane, *n*-pentane, *n*-hexane, and *n*-heptane and used to obtain conformational information.[3]

The proton NMR spectra of these straight-chain hydrocarbons are quite complicated. A two-dimensional (2D) proton NMR investigation of partially deuteriated chains yielded sets of dipolar couplings, but their large uncertainties are not suitable for extracting accurate conformational statistics,[4] as was also the case with a 2D low-resolution multiple-quantum method applied to *n*-butane.[5]

The most accurate dipolar couplings are obtained from analysis of the high-resolution proton NMR spectrum, as has been done for *n*-butane[5] and *n*-pentane.[6] The *n*-butane spectrum was initially solved by first fitting the low-resolution high-order multiple-quantum spectra, which gave excellent starting values for fitting the normal high-resolution spectrum that was obtained with excellent resolution.[5] In the case of *n*-pentane, this approach might be successful; however, the advent of high-speed computers and the development of genetic algorithms introduced new ways of solving complicated spectral problems,[7] and the first spectrum of *n*-pentane was analyzed this way.[6]

Analysis of these spectra yielded very accurate values of dipolar couplings between each pair of protons in the solute, including those between different methylene groups that are crucial for sorting out the conformational question. Analysis of these dipolar couplings indicated that effects of solvent order had only subtle effects on the solute order parameters: thus the highest possible resolution of solute dipolar couplings is desirable when attempting to extract conformational information.

There is a problem when trying to extract this conformational information from the dipolar couplings of flexible solutes that are interchanging among conformers sufficiently rapidly to produce only averaged NMR spectra (and hence dipolar couplings). The problem is that the dipolar couplings depend on the product of conformer probabilities and conformer order parameters, and these quantities cannot be separated in a straightforward manner. The normal approach has been to use a model (or assumed Hamiltonian) for the orientational order to extract conformational information. The problem is that the results then depend on the model chosen (and there are several).[8,9] To circumvent this problem, in a recent study we have noted that the orientational order parameters (as well as the anisotropic part of the intermolecular potential) for ethane and propane exhibit essentially identical temperature dependencies as solutes in the nematic phases of 5CB (4-*n*-pentyl-4′-cyanobiphenyl) and 1132 (Merck ZLI-1132). The same temperature dependence has been applied to the conformers of *n*-butane, and we were able to extract conformational information from a temperature-dependence study in the N phase.[10] In addition, the results show that the methyl CCH angle is of order 1° smaller than the one calculated with GAUSSIAN 03 MP2/cc-pvdz,[11] and this appears to be a general result for ethane,[12] propane, *n*-butane,[10] and *n*-pentane.[6]

An important aspect of conformational information is the trans−gauche energy difference that depends on three contributions to the Boltzmann factor. One is the gas-phase value, which is 643 cal mol^{-1} calculated from GAUSSIAN 03. The second arises from the effect of isotropic interactions between solute and solvent, and is of order −250 cal mol^{-1} (at 300 K) with a temperature dependence of order −2 cal mol^{-1} K^{-1}. Then there is an additional effect on the conformer populations that arises from the anisotropic intermolecular interactions; *n*-butane in the nematic solvents 5CB and 1132 gave roughly similar results.

The NMR spectra of solutes in smectic A liquid-crystal solvents have been analyzed to give orientational order parameters. Subtle changes in these order parameters are found at the nematic−smectic A (N/SmA) phase transition, and these have been analyzed using Kobayashi−McMillan (KM) theory[13,14] to yield smectic positional order parameters as well as the extent of change of the nematic potential as one progresses through a smectic layer. These studies[15−17] all involve extrapolation of the nematic potential into the smectic phase. In one case a well-studied mixture of 6OCB/8OCB (that exhibits a N phase, a SmA phase, and a low-temperature RN phase at some concentrations)[18−20] was explored. In this case the extrapolation of the nematic potential was carried out as a function of 6OCB/8OCB concentration when going from the nematic to the smectic part of the phase diagram.[17] This nematic potential is needed to fit the smectic-phase results to the KM smectic parameters κ_L' and τ', parameters that are defined below in section 3.

Here we use the 6OCB/8OCB mixture to estimate the nematic potential felt by *n*-butane in its SmA phase and wish to test the transferability of this for *n*-butane in the SmA phase of pure 8OCB, which exhibits a I−N−SmA−K phase sequence. Further, we aim to study how the smectic layering may affect the conformational averaging of hydrocarbons, and choose the simplest case of *n*-butane for investigation.

A 0.27 weight fraction 6OCB mixture of 6OCB and 8OCB (hereafter referred to as 6OCB/8OCB) is used here. This mixture has the same composition as sample 4 of ref 17 and is in the region of the phase diagram that is just inside the smectic A phase that is between N and RN phases. Thus we investigate the effects of the isotropic and anisotropic environments on the orientational and positional ordering of *n*-butane, as well as their effects on conformational averaging in the two liquid-crystal solvents that show a SmA phase.

2. EXPERIMENTAL SECTION

The solutes ethane, propane, *n*-butane, and 1,3,5-trichlorobenzene (abbreviated tcb and added to provide an orientational and chemical shift reference) were codissolved in the liquid crystal 8OCB and the mixture of 8OCB and 6OCB. Because these alkanes are gases at room temperature and ambient

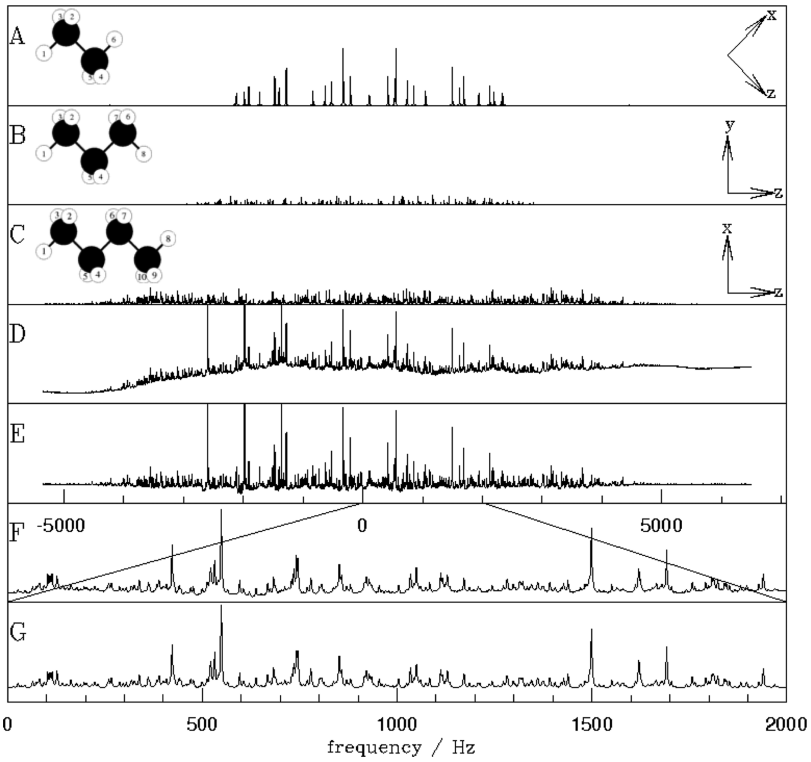

Figure 1. (A), (B) and (C) are calculated (from the fitted spectral parameters) NMR spectra of orientationally ordered alkanes. (D) is the experimental NMR spectrum of the 6OCB/8OCB liquid-crystal mixture with tcb (three largest peaks), ethane, propane, and *n*-butane codissolved at 298.0 K. (E) shows the experimental spectrum (D) after automatic baseline removal by a smoothing over 250 Hz. Trace (F) is an enlarged section of spectrum (E) compared to the calculated spectrum in (G).

pressure, they were allowed to flow into a vacuum and then condensed into an NMR tube that was prefilled with liquid crystal and tcb and submerged into liquid nitrogen. The concentrations of tcb and ethane in 8OCB are 0.4 and 1.7 mol % whereas those of *n*-butane and propane are 1.3 mol %. In the 6OCB/8OCB mixture the solute concentrations of tcb and *n*-butane were 0.4 and 0.9 mol % whereas that of ethane and propane were both 1.7 mol %. After these samples were sealed and thoroughly mixed in the isotropic phase, they were placed in turn into a Bruker Avance 400 MHz NMR spectrometer magnet. With the temperature controlled by the Bruker air-flow system, ^{1}H NMR spectra were acquired every 1, 2, or 3° from 318.0 to 343.0 K for 8OCB and from 288.0 to 345.0 K for the liquid-crystal mixture, an example of which can be found in Figure 1, which includes the calculated spectra for the alkanes.

The spectral analysis was achieved using the covariance matrix adaption evolution strategy (CMA-ES) as modified to fit the NMR spectra of multiple solutes simultaneously.[21] Performing such a task with manual peak assignment techniques would have taken a vast amount of time for the complicated and superimposed spectra, each consisting of thousands of transitions (for example panel D of Figure 1). The fitting yields very accurate sets of dipolar couplings (D_{ij}) for all solutes in the two liquid-crystal solvents as a function of temperature.

To obtain the spectral parameters defining the anisotropic spectra with an evolutionary strategy (ES), one has to first choose reasonable upper and lower limits for each parameter, which defines the search space. A complete set of spectral parameters is called a chromosome and a population of these is initially spread out randomly across the search space. To evaluate the goodness of each member of the population, a fitness function needs to be defined

$$F_{\mathbf{fg}} = \frac{(\boldsymbol{f}\cdot\boldsymbol{g})}{\|\mathbf{f}\|\,\|\mathbf{g}\|} \tag{1}$$

where **f** and **g** are the vector representations of the experimental and calculated spectra. $F_{\mathbf{fg}}$ is a measure of the extent to which a calculated spectrum overlaps with the experimental one, which is maximum at the global minimum of the error surface where the solution is obtained.[6,7,21−23] However, before all this can be done, the liquid-crystal background needs to be removed because the ES iterates on both frequency and intensity of the transitions. The usual way to remove the background in the experimental spectrum is by a manual cubic base spline, which is very time-consuming, especially when there are many spectra to be solved. This procedure can now be automated by removal of a smoothed spectrum from both the experimental and calculated spectra. The smoothed experimental spectrum $\mathbf{f}^S = (f_1^S, f_2^S, ..., f_N^S)^T$ is defined as

$$f_i^S = \frac{1}{n_S + 1} \sum_{j=i-n_S/2}^{i+n_S/2} f_j \tag{2}$$

where n_S is the number of points over which the smoothing should be performed. The smoothing over the calculated spectrum is carried out in the same way resulting in $\mathbf{g}^S = (g_1^S, g_2^S, ..., g_N^S)^T$ where

$$g_i^S = \frac{1}{n_S + 1} \sum_{j=i-n_S/2}^{i+n_S/2} g_j \tag{3}$$

dx.doi.org/10.1021/jp404315t | J. Phys. Chem. A 2013, 117, 9224−9234

The actual spectrum fitted is $\mathbf{f}^R = \mathbf{f} - \mathbf{f}^S$ against $\mathbf{g}^R = \mathbf{g} - \mathbf{g}^S$ so that $\mathbf{f}$ and $\mathbf{g}$ in eq 1 are replaced by $\mathbf{f}^R$ and $\mathbf{g}^R$. Hence the broad parts of both the experimental and calculated solute spectra that result from overlap of multiple solute lines are removed, and the broad liquid-crystal solvent spectrum is also removed from the experimental one. The idea is that removal of a smoothed spectrum removes the baseline originating from experimental sources (including the spectrum of the liquid-crystal solvent) not present in the calculated spectrum, as can be seen in Figure 1. Simultaneously, features in the spectrum that are on top of a background caused by overlapping transitions become more pronounced, so that in the global fit local features contribute more effectively to the fitness, which increases the dynamics of the fitness function. When this is done, quick convergence is observed and spectral parameters obtained. The recalculated spectra for the three alkanes together with their molecular axes are also presented in Figure 1

3. THEORETICAL BACKGROUND

In the rotational isomeric state (RIS) approximation,[24] *n*-butane exists as one of three conformers, a trans, a gauche+, or a gauche− state. There are only two independent conformers because the two gauche states are related by symmetry. The conformational distribution of *n*-butane in an anisotropic condensed phase is governed by isotropic and anisotropic contributions to the Boltzmann factor.

The isotropic part of the potential for the solute in conformer n, U_n^{iso}, is composed of the intramolecular component, $U_{int,n}^{iso}$ (which has been calculated with GAUSSIAN 03), and the intermolecular part, $U_{ext,n}^{iso}$. Therefore, the isotropic part of the trans−gauche energy difference, E_{tg}, has two contributions giving

$$E_{tg} = U_{gauche}^{iso} - U_{trans}^{iso} = E_{tg}^{int} + E_{tg}^{ext} \tag{4}$$

where $E_{tg}^{int} \equiv E_{tg}^{gas} = 643$ cal mol^{-1} is taken as the energy difference between the minima of the potential wells of trans and gauche states as calculated by GAUSSIAN 03. Values of $E_{tg}(T)$ are obtained from fits to the experimental dipolar couplings (vide infra).

If one assumes a mean-field potential for orientational ordering of the solute *s*, the order parameters for conformer n in a nematic phase can be written as

$$S_{\mu\nu}^n = \frac{\int \left(\frac{3}{2}\cos(\theta_{\mu,Z}^n)\cos(\theta_{\nu,Z}^n) - \frac{1}{2}\delta_{\mu\nu}\right)\exp(-U_n^{aniso}(\Omega_s)/kT)\,d\Omega_s}{\int \exp(-U_n^{aniso}(\Omega_s)/kT)\,d\Omega_s} \tag{5}$$

where $\theta_{\mu,Z}^n$ is the angle between the μ-molecular axis of the nth conformer and the nematic director, which for experiments herein is aligned along the magnetic field (Z) direction. Here $U_n^{aniso}(\Omega_s)$ is taken to be the classic Maier−Saupe potential $H_{N,Ls}^n(\Omega_s)$,[25,26] which has been shown to be very successful for the description of the orientational order of solutes (s) in nematic liquid crystals (L).[27] For a solute of general symmetry in conformation n and in an axially symmetric nematic mean-field, the Hamiltonian can be written as

$$U_n^{aniso}(\Omega_s) \equiv H_{N,Ls}^n(\Omega_s) = -\frac{3}{4}G_{L,ZZ}\sum_\mu\sum_\nu \cos(\theta_{\mu,Z}^n)\cos(\theta_{\nu,Z}^n)\beta_{\mu\nu}^n(\text{solute}) \tag{6}$$

where $\beta_{\mu\nu}^n$(solute) is the $\mu\nu$ anisotropic part of some electronic solute molecular property. $G_{L,ZZ}$ (hereafter written G_L) is the ZZ component of the liquid-crystal field and is related to the solvent (L) nematic order parameter $S_{L,ZZ}$ with the Z axis being the mean-field symmetry axis.

In a smectic phase, the solute would feel (in addition to the nematic mean field) the effect of layering (smectic order) and its coupling with the nematic ordering. The layering in SmA phases can be described by Kobayashi−McMillan theory.[13,14] Now $U_n^{aniso}(\Omega_s,Z)$ has two additional terms, one describing the periodic layering specified by an interaction strength prefactor τ_n' and the second being a coupling term between nematic orientational and smectic layering potentials with a prefactor κ_L'. The potential exerted on the solute in a smectic phase is given by

$$U_n^{aniso}(\Omega_s,Z) \equiv H_{A,Ls}^n(\Omega_s,Z) = H_{N,Ls}^n(\Omega_s)\left(1 + \kappa_L'\cos\left(\frac{2\pi Z}{d}\right)\right) - \tau_n'\cos\left(\frac{2\pi Z}{d}\right) \tag{7}$$

where the prefactor κ_L' can in principle be temperature dependent, whereas the solute smectic prefactor τ_n' is the coupling strength for a solute to feel the smectic layering of the solvent molecules. The layer width is d whereas Z ($Z = 0$ in the center of a layer) is along the layer normal.

The solute orientational order parameters of eq 5 can be calculated in each phase using either eq 6 for $U_n^{aniso}(\Omega_s)$ or eq 7 for $U_n^{aniso}(\Omega_s,Z)$ (with additional integration over Z from 0 to d). The D_{ij} that are obtainable from analysis of the NMR spectra are functions of these orientational order parameters

$$D_{ij} = \sum_n p^n \sum_{k,l} d_{kl,ij}^n S_{kl}^n \tag{8}$$

where $d_{kl,ij}^n$ is given by

$$d_{kl,ij}^n = -\frac{h\gamma_i\gamma_j}{4\pi^2}(\cos\alpha_{ij,k}^n\cos\alpha_{ij,l}^n/r_{n,ij}^3) \tag{9}$$

with $\cos\alpha_{ij,k}^n$ the cosine of the angle between the ij direction in the molecule in conformation n, and k a conformer-fixed axis.

The probability of conformer n (p^n) is a function of both the isotropic (U_n^{iso}) and anisotropic (U_n^{aniso}) parts of the potential and can be written

$$p^n = \frac{\sqrt{I_{xx}^n I_{yy}^n I_{zz}^n}\exp(-U_n^{iso}/kT)\int d\Omega_s\int_0^Z dZ\exp(-U_n^{aniso}(\Omega_s,Z)/kT)}{\sum_n\sqrt{I_{xx}^n I_{yy}^n I_{zz}^n}\exp(-U_n^{iso}/kT)\int d\Omega_s\int_0^Z dZ\exp(-U_n^{aniso}(\Omega_s,Z)/kT)} \tag{10}$$

where $(I_{xx}^n I_{yy}^n I_{zz}^n)^{1/2}$ is a rotational kinetic energy factor that is dependent on the principal values of the moment of inertia tensor for each conformer.[2] The integral over Z is only needed for SmA-phase spectra.

Hence, a least-squares fit to the experimental D_{ij} allows us to determine the prefactors in the smectic potential (eq 7) provided that one has prior knowledge of $H_{N,Ls}^n$ at the temperature of interest in the SmA phase. Fortunately, the product $G_L\beta_{\mu\nu}$(solute) of alkanes can in principle be determined in the nematic phase (vide infra). For each conformer of *n*-butane at each temperature in each liquid crystal there are three product $G_L\beta_{\mu\nu}^n$(*n*-butane) energy parameters. For *n*-butane in the mixture we abbreviate these

dx.doi.org/10.1021/jp404315t | J. Phys. Chem. A 2013, 117, 9224−9234

parameters to $G_L\beta^n_{xx}$, $G_L\beta^n_{yy}$, and $G_L\beta^n_{xy}$, and these are needed to give the nematic potential in a smectic phase. In the present case, these have been obtained from fits to experiments performed in the nematic phases on a sample (6OCB/8OCB) that exhibits both a N phase above and a RN nematic phase below the SmA phase. Values for the smectic A phase are then obtained by interpolation of the nematic-phase ethane values. Once the full smectic potential $H^n_{A,Ls}(\Omega_s,Z)$ is known, the solute smectic order parameter τ^n can be easily evaluated according to

$$\tau^n = \frac{\int d\Omega_s \int_0^d \cos\left(\frac{2\pi Z}{d}\right) e^{-H^n_{A,Ls}(\Omega_s,Z)/kT}\, dZ}{\int d\Omega_s \int_0^d e^{-H^n_{A,Ls}(\Omega_s,Z)/kT}\, dZ} \quad (11)$$

The κ^n_{Ls} order parameters (for κ'_L coupling) can in principle be calculated for each solute, but there are many of them and they seem not to give additional insight like the translational order parameter τ.

4. RESULTS AND DISCUSSION

The dipolar couplings for the four solutes tcb, ethane, propane, and *n*-butane obtained using CMA-ES for spectral analysis as a function of temperature in the liquid-crystal solvents 8OCB and 6OCB/8OCB are reported in the Supporting Information. Parameters calculated from or fitting to these dipolar couplings are reported in Figure 2 for $G_L\beta_{zz}$(ethane) (hereafter written $G\beta_{ethane}$) and in Table 1 where we include E_{tg} and its temperature variation, the change in CCH angle for *n*-butane, and the ratios of $G_L\beta_{\mu\nu}$ parameters to those for ethane. Below, we first describe how we obtain the $G\beta_{ethane}$ from the spectral parameters. Next we check that for the liquid crystals used here the propane energy parameters scale to those for ethane. We then use this scalability to obtain the $G_L\beta^n_{\mu\nu}$ parameters for butane, as well as conformer probabilities. The parameters obtained for the mixture are used to fit the spectra from 8OCB with no adjustable parameters. For all solutes we use the parameters obtained for the N and RN phases of the mixture to analyze results in the SmA phase to obtain the smectic prefactors and the smectic order parameters τ.

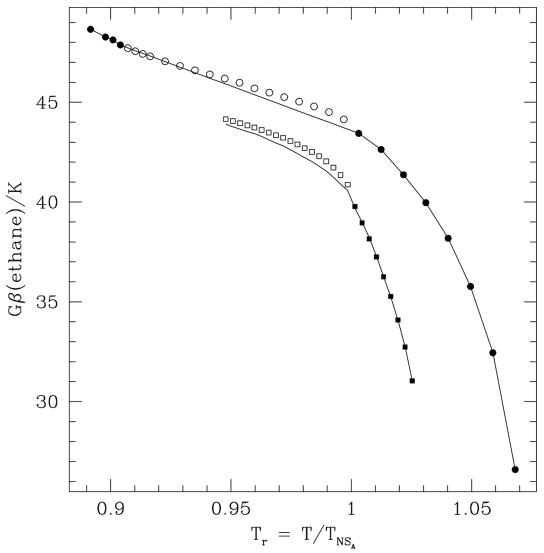

Figure 2. $G\beta_{ethane}$ as a function of reduced temperature for the 6OCB/8OCB mixture (circles) and 8OCB (squares). Symbols: filled points, nematic or reentrant-nematic phases; open points, smectic A phases. The line for 6OCB/8OCB is a spline fit to the nematic and reentrant-nematic points only with interpolation in the smectic phase given by a straight line connecting the lowest temperature N and highest temperature RN points. The line for the 8OCB sample in the smectic phase is drawn using the relative shift of $G\beta_{ethane}$ from the 6OCB/8OCB sample at the same reduced temperature. The smectic potential is not included in the calculation.

Table 1. Parameters Obtained from Analysis of Experimental Dipolar Couplings from Spectra of Nematic and Reentrant-Nematic Phases of 6OCB/8OCB

parameter	RIS	continuous potential
n-Butane in 6OCB/8OCB[a,b]		
$E_{tg}(300)$/cal mol^{-1} (at T = 300 K)	400 ± 23	336 ± 15
E'_{tg}/cal mol^{-1} K^{-1}	−0.71 ± 0.07	−1.28 ± 0.06
CCH decrease/deg	0.64 ± 0.04	0.79 ± 0.03
$G_L\beta^{trans}_{zz}/G\beta_{ethane}$	4.30 ± 0.07	4.32 ± 0.04
$G_L\beta^{trans}_{xx}/G\beta_{ethane}$	−1.60 ± 0.03	−1.70 ± 0.02
$G_L\beta^{trans}_{xz}/G\beta_{ethane}$	0.02 ± 0.01	−0.03 ± 0.01
$G_L\beta^{gauche}_{zz}/G\beta_{ethane}$	1.78 ± 0.03	1.79 ± 0.02
$G_L\beta^{gauche}_{xx}/G\beta_{ethane}$	−1.04 ± 0.07	−1.47 ± 0.05
$G_L\beta^{gauche}_{xz}/G\beta_{ethane}$	−0.08 ± 0.01	0.07 ± 0.01
RMS[c]/Hz	2.7	1.9
Propane		
$G_L\beta_{xx}$(propane)/$G\beta_{ethane}$	−1.2806 ± 0.0001	
$G_L\beta_{yy}$(propane)/$G\beta_{ethane}$	−0.5855 ± 0.0003	
RMS[c]/Hz	0.6	

[a]When the parameters obtained for the 6OCB/8OCB sample reported in this table are used to calculate with no adjustable parameters the dipolar couplings for the nematic-phase points in the 8OCB sample, the RMS difference between experimental and calculated dipolar couplings is 2.7 and 2.1 Hz for the RIS and the continuous potential calculations. [b]E_{tg} of eq 4 = $E_{tg}(300) + E'_{tg}(T - 300\ K)$ [c]The RMS are the root-mean-square differences between the experimental nematic-phase D_{ij} and those calculated with the fitting parameters.

4.1. Ethane.

The two independent dipolar couplings from each ethane spectrum are used to calculate the order parameter S_{zz} for the c_3 symmetry axis of ethane and the CCH angle. The fitted value of the CCH angle is 0.60° smaller than the experimental value. This decrease is consistent with earlier investigations when effects of internal motions and nonrigid effects are neglected.[12,28,29] The order parameter is used with eq 6 to find the product $G\beta_{ethane}$. The results are displayed as circles for the 6OCB/8OCB sample and squares for the 8OCB sample in Figure 2 where the filled symbols are for results in the N and RN phases and the open symbols are smectic A phases. There is a break in the smooth variation with reduced temperature ($T_r = T/T_{SmA/N}$) of the points at the SmA/N-phase transition temperature ($T = T_{SmA/N}$), indicative of a small effect of the smectic phase, similar to effects observed for solutes in earlier studies.[15−17,21,30,31]

For 6OCB/8OCB, in keeping with past practice, we do a spline fit on the N and RN points only, and the resulting interpolated points in the SmA phase can be represented by a straight line. Hence, for 6OCB/8OCB the line represents the anisotropic nematic ordering in all phases. At this stage, eqs 5 and 7 are used to fit the ethane order parameter in 6OCB/8OCB using the $G\beta_{ethane}$ given by the line for the SmA phase and adjusting τ' as the only fitting parameter.

dx.doi.org/10.1021/jp404315t | J. Phys. Chem. A 2013, 117, 9224−9234

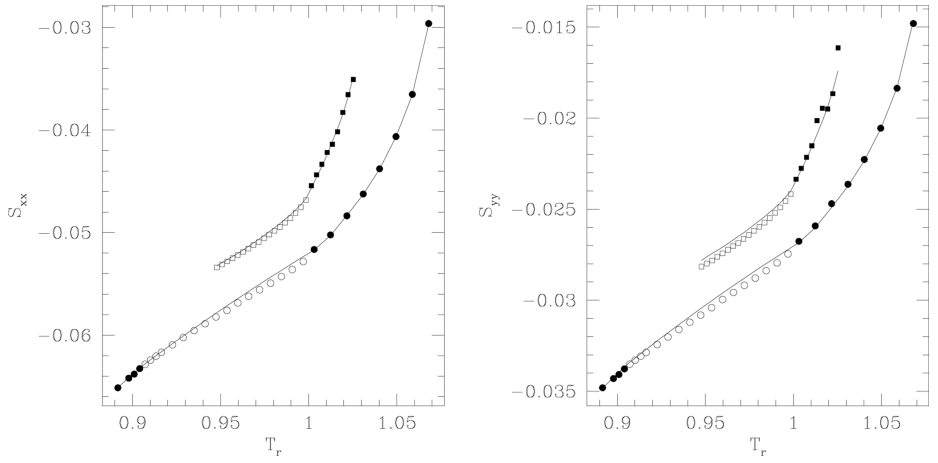

Figure 3. Points: experimental propane orientational order parameters. Lines: calculated using the nematic potential only with the $G\beta_{ethane}$ of Figure 2 and the scaling factors (in Table 1) $\beta_{xx}(propane)/\beta_{ethane}$ and $\beta_{yy}(propane)/\beta_{ethane}$ obtained from the fit to the propane D_{ij} in the nematic and reentrant-nematic phases of the 6OCB/8OCB sample. Symbols: 6OCB/8OCB mixture, circles; 8OCB, squares. Nematic-phase points are filled, whereas smectic A phase points are open. The calculated line for the 8OCB sample uses the β ratios from the 6OCB/8OCB sample and involves no adjustable parameters.

Note that throughout this paper we fix the value of κ'_L in eq 7 for all alkanes in 6OCB/8OCB and 8OCB to the average value 0.277 ± 0.02 obtained in an earlier study using different solutes in the same liquid-crystal solvent.[17] In this earlier study, two nematic potentials were included, interaction 1 being attributed to short-range size and shape effects, and interaction 2 to the anisotropy in longer-range electrostatic interactions such as those involving molecular polarizabilities or quadrupole moments. However, the solutes we investigate here (except tcb) are taken to be "magic solutes", meaning that the longer-range electrostatic interactions are assumed to be of minor importance and can be neglected.[32] Hence here we assume the second mechanism plays no role, and use the value of κ'_L for the first mechanism. The positional order parameters τ^{ethane} calculated from eq 11 are presented below.

In the case of the 8OCB sample in Figure 2, the line is drawn by applying the same relative change in $G\beta_{ethane}$ as was used at the same reduced temperature in the linear interpolation for 6OCB/8OCB. In what follows, the $G\beta_{ethane}$ values represented by the lines are used for analysis of the solutes propane and *n*-butane. We emphasize that the lines in the nematic phases have only one single adjustable parameter ($G\beta_{ethane}$) for each temperature, and in the smectic phase the lines are based on interpolation between the N and RN phases of 6OCB/8OCB: the smectic-phase Hamiltonian of eq 7 is not used in generating Figure 2.

4.2. Propane. Next we check the scalability of ethane to propane anisotropic energy parameters in the two solvents used here. First, for each spectrum we adjust the two independent propane orientational order parameters S_{xx} and S_{yy} in a fit to the four experimental dipolar couplings obtained at each temperature. The CCH angle decrease was also fitted, and precisely the same value (0.60°) as found for ethane was obtained. The order parameters obtained from this fit are displayed as circles (6OCB/8OCB) and squares (8OCB) in Figure 3, using filled symbols for nematic-phase and open symbols for smectic-phase values. In these fits the RMS difference between experimental and recalculated dipolar couplings was 0.3 Hz for 6OCB/8OCB and 1.2 Hz for 8OCB.

We next adjust the two energy-parameter ratios $\beta_{xx}(propane)/\beta_{ethane}$ and $\beta_{yy}(propane)/\beta_{ethane}$ in a fit to the propane order parameters (from the above fit) of the 6OCB/8OCB N and RN results (see Table 1 for results). The low RMS indicates the excellent scalability of ethane to propane energy parameters. The order parameters recalculated from these two fitting parameters agree exceedingly well in the nematic phases with the experimental values for both liquid crystals investigated here (lines through the nematic-phase points in Figure 3). The calculation of the 8OCB order parameters uses the β ratios from the 6OCB/8OCB fit and involves no adjustable parameters. As was the case for the liquid crystals 5CB and 1132, the propane and ethane energy parameters scale to each other.[10]

We mention that a similar scaling does not apply to the tcb (dipolar couplings obtained from the same spectra and reported in the Supporting Information), which indicates that a second, different mechanism is needed in conjunction with the two Maier−Saupe potential to rationalize the tcb results.

It is interesting to note that the β ratios obtained agree reasonably well with those for interaction 1 ($\beta_{xx}(propane)/\beta_{ethane} = -1.15$, $\beta_{yy}(propane)/\beta_{ethane} = -0.55$, where values refer to the axis systems used in this paper) from a two Maier−Saupe potential applied to a number of solutes in a variety of different liquid-crystal solvents.[27]

We note that the line and points do not coincide in the smectic phases in Figure 3. This is mainly because the nematic potential used is the one generated from the interpolated 6OCB/8OCB smectic results of Figure 2, which also differed from the experimental points for ethane. When the smectic-phase Hamiltonian (eq 7) is used with τ' as the only fitting parameter for each temperature, the agreement between experimental and calculated orientational order parameters is excellent. The smectic-phase $\tau^{propane}$ order parameters calculated from eq 11 are discussed below.

4.3. *n*-Butane. The results for ethane and propane show that the anisotropic ordering potential for propane is proportional to that for ethane in the nematic phases of both liquid crystals investigated here. As in the earlier study, we now assume that the same applies to the conformers of longer-chain hydrocarbons, with *n*-butane the first and simplest example.

When we compare *n*-butane dipolar couplings with those of ethane (or propane), the differing t, g+, and g− conformer

dx.doi.org/10.1021/jp404315t | J. Phys. Chem. A 2013, 117, 9224−9234

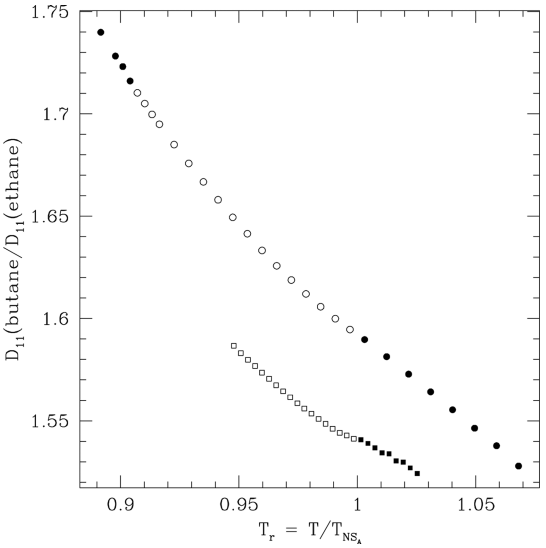

Figure 4. D_{11}(butane)/D_{11}(ethane) as a function of reduced temperature for the 6OCB/8OCB mixture (circles) and the 8OCB sample (squares). Nematic-phase points are filled, whereas smectic A phase points are open. D_{11} is the intramethyl proton−proton coupling.

populations show up as a temperature dependence in the ratio, as shown for D_{11}(butane)/D_{11}(ethane) in Figure 4. Similar effects are seen for other *n*-butane dipolar couplings. There is a break in the smooth curve of the N phase at the SmA/N phase transition for both liquid crystals, and this break is most easily seen in Figure 4 for the 8OCB sample. Such a discontinuity, albeit very small, is an indication of some effect of the smectic layering on the *n*-butane conformers, either their populations or their dipolar couplings. The main effect in the figure (the change in coupling ratios with temperature) is caused by the population differences with temperature; the 8OCB and 6OCB/8OCB ratios differ at the SmA/N phase transition because this occurs at different real temperatures.

4.3.1. Nematic and Reentrant Nematic Phases of the 6OCB/8OCB Sample, RIS Approximation. To proceed, we start with 6OCB/8OCB and fit to the seven dipolar couplings obtained from the analysis of each *n*-butane spectrum. First, as for propane, we assume that the anisotropic potential for each *n*-butane conformer is proportional to the $G\beta_{\text{ethane}}$ obtained from the same spectrum and plotted in Figure 2. The symmetry (C_{2h}, trans and C_2, gauche) of the RIS conformers demands three anisotropic energy parameters for each *n*-butane conformer, being $G_1\beta^n_{xx}$, $G_1\beta^n_{zz}$, and $G_1\beta^n_{xz}$. Thus there are six adjustable ratios, three for trans and three for gauche conformers. In addition, we adjust the methyl CCH angle and the E_{tg} of eq 4 and include a linear temperature dependence of E_{tg} with coefficient E'_{tg} (as was found helpful in the earlier study[10]). The fit is performed to all N and RN *n*-butane dipolar couplings from 6OCB/8OCB, and the RMS difference between experimental and fitted dipolar couplings for the fit to 8 N and 4 RN spectra with only nine adjustable parameters is 2.7 Hz. This RMS is impressive for fitting to straight-chain hydrocarbons over the 57 K temperature range (288−345 K), especially considering that, except for the CCH methyl angle, the geometry used is that calculated from GAUSSIAN 03, and various nonrigid effects[29] are ignored.

The orientational order parameters of the *n*-butane conformers are calculated in these fits and are displayed by the filled circles in Figure 5 in terms of S^n_{zz} (the order parameter for the principal ordering axis) and η_n (=$(S^n_{xx} - S^n_{yy})/S^n_{zz}$, the asymmetry in the order matrix for conformer *n*). Values of the angle between the principal moment of inertia (PMI) and principal ordering (POA) axes are given in the figure caption. The parameters obtained from the fit are given in column RIS of Table 1. The results agree quite favorably with those of the earlier study of *n*-butane in the liquid crystals 5CB and 1132, where for example the same calculation (UT of Table 2) gave E_{tg} values of 481 and 340 cal mol^{-1} for 5CB and 1132.[10]

The *n*-butane conformers in the above calculation are taken to be rigid (except for rotation of the methyl groups about their

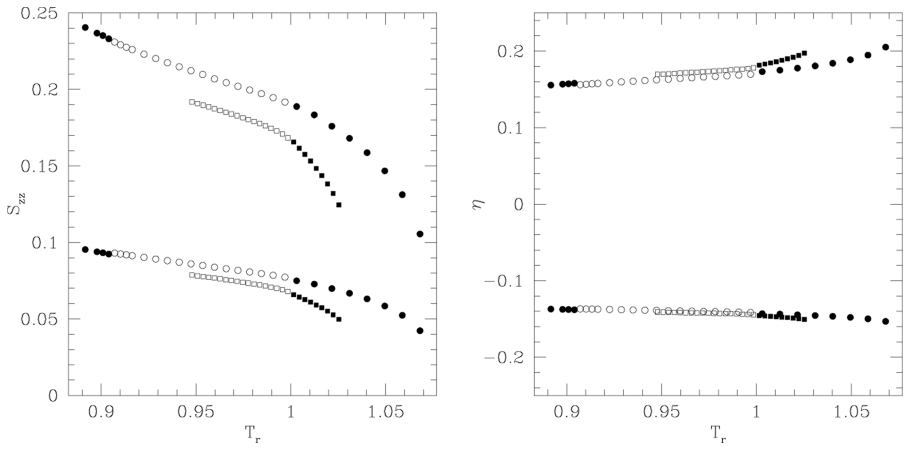

Figure 5. *n*-Butane order parameters (calculated from the RIS approximation) for principal ordering direction and asymmetry in order-parameter matrix, all calculated using the potential of eq 7 with κ'_L set equal to 0 ($\tau'_n = 0$) for the nematic phase and 0.277 for the smectic A phase. The $G_1\beta^n_{\mu\nu}$ parameters of the nematic term $H^n_{N,Ls}(\Omega_s)$ (see eq 6) are calculated from the ethane $G\beta_{\text{ethane}}$ spline-fit line in Figure 2 and the $G\beta$ ratios of Table 1. Symbols: filled symbols, nematic phases; open symbols, smectic phase; circles, 6OCB/8OCB; squares, 8OCB. The upper points are results for the trans conformer, and the lower ones are for the gauche. The diagonalization angle between the PMI and POA axes (positive for clockwise rotation of the PMI axis about the *y* c_2 symmetry axis for the structure displayed in Figure 1, and the same for all spectra) is −0.17° for the trans and −1.70° for the gauche conformer. When the full potential (integration over all dihedral angles) is used for the calculations, the values obtained for S_{zz} and η are unchanged, but the diagonalization angles are now +0.33° and −1.14° for trans and gauche conformers. All smectic-phase calculations (open symbols) have τ'_n as the only adjustable parameter.

dx.doi.org/10.1021/jp404315t | J. Phys. Chem. A 2013, 117, 9224−9234

c_3 axes): the RIS approximation does not account for libration about the dihedral angle.

4.3.2. Nematic and Reentrant Nematic Phases of the 6OCB/8OCB Sample, Continuous Torsional Potential. To investigate the consequence of the "normal" RIS approximation, we also performed fits to the NMR results taking into account rotation about the central C−C bond in 5° steps, referred to as "full potential fits" in Table 3 of ref 10. The potential energy for each dihedral angle is calculated with GAUSSIAN 03 assuming the structure (except the dihedral angle) in each potential well is identical to that calculated at the well minimum, and a single set of $G\beta$ parameters is used for each well. The resulting parameters are quite similar (Table 1), but as was the case with the earlier study, the value obtained for E_{tg} is smaller than with the RIS approximation. It is noteworthy that the RMS of the fit is now reduced to 1.9 Hz. The S_{zz} and η parameters obtained for each conformer at each temperature are almost identical to those values obtained for the RIS calculation (Figure 5), but the diagonalization angles differ (see caption to Figure 5).

4.3.3. Smectic A Phase of 6OCB/8OCB Sample. Now that we have an excellent fit to the *n*-butane couplings in the nematic phases of 6OCB/8OCB, we use the $G_L\beta^n_{\mu\nu}/G\beta_{ethane}$, E_{tg}, E'_{tg}, and CCH angle parameters obtained from that fit and examine the SmA-phase results for 6OCB/8OCB. This time we fit individual spectra by adjusting only τ'_n. In each case the RMS of the difference between experimental and recalculated dipolar couplings is on the order of 2.3 Hz, indicating a fit quality equivalent to that obtained for the nematic-phase results above. The orientational order parameters obtained are the open circles in Figure 5, and the positional order parameters calculated from the fitted τ'_n are discussed below.

4.3.4. Nematic and Smectic A Phases of the 8OCB Sample. We now turn to the 8OCB sample. We use the ethane $G\beta_{ethane}$ from the line for 8OCB in Figure 2 for each spectrum, and take the six $G\beta$ ratios, E_{tg}, and CCH decrease parameters found in the fits to *n*-butane in the nematic phases of 6OCB/8OCB (Table 1) to calculate the dipolar couplings for each spectrum in the nematic phase of 8OCB. The RMS deviation of this calculation, with no adjustable parameters, is 2.7 Hz, exactly the same as the actual fit to the nematic results of 6OCB/8OCB! This result is astounding and is a strong indication that: the couplings scale among hydrocarbons, including their conformers; the same mechanism is operating in 8OCB and 6OCB/8OCB, indicating that indeed these hydrocarbons are "magic solutes"; and this single mechanism is likely associated with size and shape (i.e., entropic effects).

Next we consider the smectic-phase results for 8OCB to determine τ'_n. As above, we use the $G\beta_{ethane}$(8OCB) from the 8OCB line in Figure 2 and the nematic $G_L\beta^n_{\mu\nu}/G\beta_{ethane}$, E_{tg}, E'_{tg}, and CCH angle decrease parameters from the 6OCB/8OCB results in Table 1. The order parameters calculated with no adjustable parameters from the individual fit to each 8OCB smectic-phase spectrum are displayed as open squares in Figure 5, and the positional order parameters calculated from the fitted τ'_n are discussed below. The RMS of these fits is 1.6 Hz.

4.4. Probabilities. A main interest of this investigation is the relative populations and the factors that contribute to the populations of the trans and gauche conformers. The values of E_{tg} (eq 4) obtained from the fit to the nematic-phase results for 6OCB/8OCB include E^{int}_{tg} (the gas-phase value) plus E^{ext}_{tg} (the isotropic condensed-phase energy difference). Hence for the results reported here E^{ext}_{tg} is negative and therefore increases the gauche population over that for the gas phase. The probability of the trans conformer calculated using this combined isotropic value E_{tg} in the Boltzmann factor along with the inertial factor gives the results displayed by the lines in Figure 6. These lines differ between 6OCB/8OCB and 8OCB only because of the different $T_{SmA/N}$ values for the two liquid crystals; if plotted versus T, they would overlap.

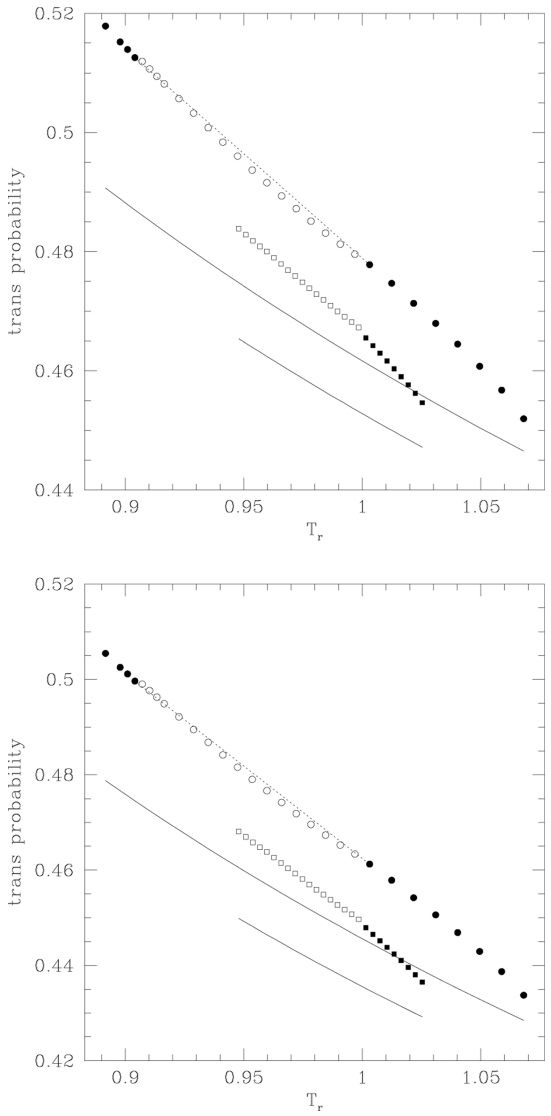

Figure 6. Probability of *trans-n*-butane conformer as a function of reduced temperature. RIS, top; full potential (integration over all dihedral angles), bottom; filled symbols, N and RN; open symbols, SmA; circles, 6OCB/8OCB; squares, 8OCB; lines, calculation using isotropic potential only; symbols, calculations (using eq 7 including anisotropic intermolecular orientational and positional interactions, with integration over Z in the SmA phase) with RIS (top) or the full C−C bond torsional potential (bottom). The dotted line is a smooth curve connecting the N and RN phases.

The effect of the ordered phases on the probabilities is readily seen in Figure 6 by the greater trans probabilities found when the anisotropic potential is included in the calculation of probabilities as per eq 10. The gap between isotropic and full potential probabilities increases to lower temperature because the anisotropic potential increases.

dx.doi.org/10.1021/jp404315t | J. Phys. Chem. A 2013, 117, 9224−9234

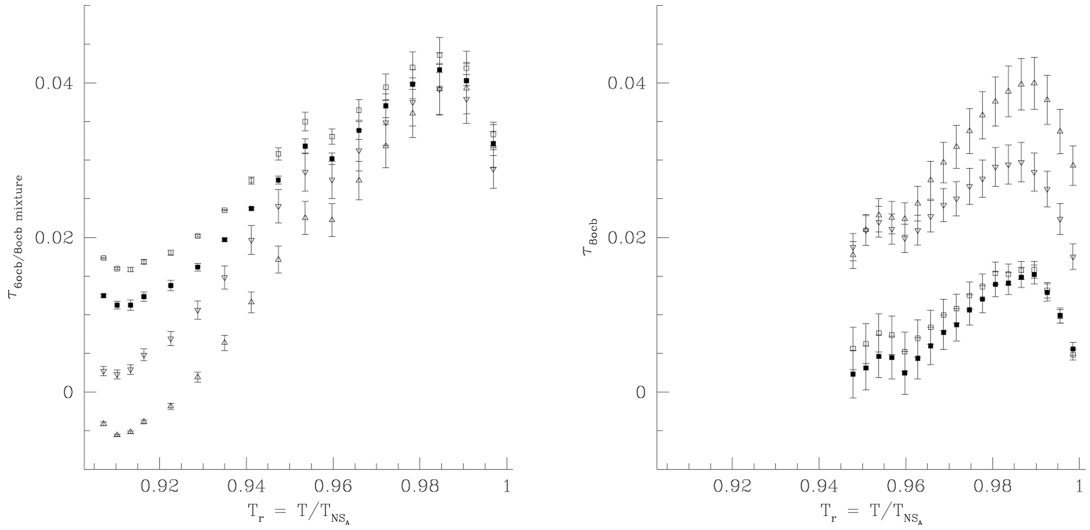

Figure 7. Positional order parameter τ (calculated from eq 11) as a function of reduced temperature for the 6OCB/8OCB mixture (left) and 8OCB (right); ethane, up-triangles; propane, down-triangles; *n*-butane, open squares, RIS; *n*-butane, filled squares, full potential (integration over all dihedral angles). The error limits displayed reflect the limits of $\kappa'_L = 0.277 \pm 0.02$ from ref 17.

The presence of the smectic phases introduces some subtle features into Figure 6. For the 8OCB sample, there is a break in the slope of the probability versus T_r curve at $T = T_{SmA/N}$. A smaller break is also seen for 6OCB/8OCB, and the smooth curve connecting the N and RN phases (dotted line) lies above the experimental points that curve back up toward this dotted line as the RN phase is approached. Thus, not only does the orientational ordering affect the conformer populations, but also the layering in the smectic A phase contributes (albeit a rather small effect). The lower trans population in the SmA phase indicates that the gauche conformer may be better accommodated in the interlayer region of the SmA phase than it is in the nematic phase.

4.5. Smectic Order Parameter. The values of τ' (taken to be a property of both the solvent and the solute) along with the assumed value of κ'_L (taken to be a constant liquid-crystal property) from the fits above to the measured dipolar couplings in the smectic A phases of the liquid-crystal samples can be used with eq 11 to calculate the layering order parameter τ for each solute in each experiment. For *n*-butane the weighted averages of values calculated for the individual conformers are used. The results are displayed in Figure 7. In general, τ is small and positive. The error bars reflect the RMS of the κ'_L values from ref 17. Considering that the nematic potential depends on the line interpolated between N and RN phases in 6OCB/8OCB, the changes in τ values with temperature, with sample, and with solute are not considered significant. The small values indicate there is not much partitioning of the solutes in the smectic layers, and the positive value indicates a slight preference for these hydrocarbon solutes to partition within the smectic layers.

5. CONCLUSION

The use of evolution strategies for the fitting of very complicated NMR spectra has made it feasible to perform a comprehensive temperature study of the three molecules, ethane, propane, and *n*-butane, codissolved in two different liquid-crystal phases. Correcting the baseline to remove the broad liquid-crystal spectrum is no longer needed when smoothed experimental spectra are compared with smoothed calculated ones. Being able to fit simultaneously the spectra of the three solutes in the same sample tube removes the problem of comparing results from different samples, a procedure that is fraught with error because of the large dependence of solute ordering on sample conditions, including temperature and concentration.

The dipolar couplings and anisotropic energy parameters of ethane and propane scale to each other, which suggests that the same scaling will apply to the *n*-butane conformers. Using this approximation, the fitting of all *n*-butane spectral parameters in the N and RN phases of 6OCB/8OCB reduces to only nine fitting parameters, being the six energy scaling parameters (three $G_L\beta^n_{\mu\nu}/G\beta_{ethane}$ for each of gauche and trans), E_{tg}, E'_{tg}, and the CCH angle decrease needed to account for the neglect of nonrigid effects (except for methyl-group rotations and changing dihedral angle). The resulting RMS between experimental and calculated dipolar couplings is only 2.7 Hz. When a more complete approach is used for rotation about the central C−C bond in *n*-butane (integration over the dihedral angle instead of using the three-state RIS approximation), the RMS reduces to 1.9 Hz. These nine parameters along with the $G\beta_{ethane}$ for each spectrum from Figure 2 are then used to predict the dipolar couplings obtained from the 8OCB sample. The fits with no adjustable parameters to the nematic-phase *n*-butane couplings in the 8OCB samples are 2.7 Hz (RIS) and 2.1 Hz (full potential). These absolutely amazing results attest to the validity of the energy-parameter scaling, the accuracy of structure calculated by GAUSSIAN 03, and the general approach used.

The effect of the SmA phase on the spectral parameters is rather subtle but can be seen in the various graphs. When we take the value of the κ'_L coupling prefactor from an earlier work, we can fit all spectra in the SmA phase to a single adjustable parameter τ' for each solute in each liquid crystal at each temperature, which is then used to calculate the smectic order parameter τ. The values obtained indicate that the three solutes ethane, propane, and *n*-butane do not show a large partitioning in the smectic phase but do have a slight preference for the interlayer region of that phase.

dx.doi.org/10.1021/jp404315t | J. Phys. Chem. A 2013, 117, 9224−9234

The conformational averaging of hydrocarbon chains, sometimes called their flexibility, is affected by intramolecular interactions (the only important ones in the gas phase), isotropic intermolecular interactions between the hydrocarbon and its surroundings, and the anisotropic interactions between solute and anisotropic environment, including orientational and positional effects. The results of this study show that the gauche conformer probability is enhanced by isotropic interactions in the condensed phase. The trans probability is enhanced by the anisotropic orientational part of the intermolecular potential, which makes intuitive sense in that a more elongated solute is likely more easily accommodated in a nematic-type environment. We found that the population of the gauche conformer in the SmA phase is slightly enhanced over that expected for a nematic phase.

■ ASSOCIATED CONTENT

Supporting Information

Dipolar couplings for ethane, propane, *n*-butane and tcb in 6OCB/8OCB and in 8OCB samples. This information is available free of charge via the Internet at http://pubs.acs.org.

■ AUTHOR INFORMATION

Corresponding Author

*E. E. Burnell: e-mail, elliott.burnell@ubc.ca; homepage, http://www.chem.ubc.ca/our-people/profiles/elliott-burnell-0.

Notes

The authors declare no competing financial interest.

[§]A. C. J. Weber: e-mail, webera@brandonu.ca; homepage, http://people.brandonu.ca/webera/.

[†]R. Y. Dong: e-mail, rondong@phas.ubc.ca.

[‡]W. L. Meerts: e-mail, leo.meerts@science.ru.nl; homepage, http://www.leomeerts.nl.

■ ACKNOWLEDGMENTS

E. E. Burnell and R. Y. Dong thank the Natural Sciences and Engineering Research Council of Canada for financial support.

■ REFERENCES

(1) Photinos, D. J.; Samulski, E. T.; Toriumi, H. Alkyl Chains in a Nematic Field. 1. A Treatment of Conformer Shape. *J. Phys. Chem.* **1990**, *94*, 4688−4694.

(2) Photinos, D. J.; Samulski, E. T.; Toriumi, H. Alkyl Chains in a Nematic Field. 2. Temperature and Chain Length Dependence of Orientational Ordering. *J. Phys. Chem.* **1990**, *94*, 4694−4700.

(3) Tynkkynen, T.; Hassinen, T.; Tiainen, M.; Soininen, P.; Laatikainen, R. ^{1}H NMR Spectral Analysis and Conformational Behavior of n-alkanes in Different Chemical environments. *Magn. Reson. Chem.* **2012**, *50*, 598−607.

(4) Rosen, M. E.; Rucker, S. P.; Schmidt, C.; Pines, A. Two-Dimensional Proton NMR Studies of the Conformations and Orientations of n-Alkanes in a Liquid-Crystal Solvent. *J. Phys. Chem.* **1993**, *97*, 3858−3866 and references therein.

(5) Polson, J. M.; Burnell, E. E. Conformational Equilibrium and Orientational Ordering: ^{1}H Nuclear Magnetic Resonance of Butane in a Nematic Liquid Crystal. *J. Chem. Phys.* **1995**, *103*, 6891−6902.

(6) Meerts, W. L.; de Lange, C. A.; Weber, A. C. J.; Burnell, E. E. Evolutionary Algorithms to Solve Complicated NMR Spectra. *J. Chem. Phys.* **2009**, *130*, 044504−044504-8.

(7) Meerts, W. L.; Schmitt, M. Application of genetic algorithms in automated assignments of high-resolution spectra. *Int. Rev. Phys. Chem.* **2006**, *25*, 353−406.

(8) Weber, A. C. J.; de Lange, C. A.; Meerts, W. L.; Burnell, E. E. The Butane Condensed Matter Conformational Problem. *Chem. Phys. Lett.* **2010**, *496*, 257−262.

(9) Weber, A. C. J.; Burnell, E. E. Conformational Statistics of n-Butane in the Condensed Phase and the Effects of Temperature. *Chem. Phys. Lett.* **2011**, *506*, 196−200.

(10) Burnell, E. E.; Weber, A. C. J.; de Lange, C. A.; Meerts, W. L.; Dong, R. Y. Nuclear Magnetic Resonance Study of Alkane Conformational Statistics. *J. Chem. Phys.* **2011**, *135*, 234506−234506-10.

(11) Frisch, M. J.; Trucks, G. W.; Schlegel, H. B.; Scuseria, G. E.; Robb, M. A.; Cheeseman, J. R.; Montgomery, J. A., Jr.; Vreven, T.; Kudin, K. N.; Burant, J. C.; et al. *Gaussian 03*, Revision B.05; Gaussian, Inc.: Pittsburgh, PA, 2003.

(12) Burnell, E. E.; de Lange, C. A. NMR as a Tool in the Investigation of Fundamental Problems in Ordered Liquids. *Solid State NMR* **2005**, *28*, 73−90.

(13) Kobayashi, K. K. Theory of Translational and Orientational Melting with Application to Liquid Crystals. *Mol. Cryst. Liq. Cryst.* **1971**, *13*, 137−148.

(14) McMillan, W. L. Simple Molecular Model for the Smectic A Phase of Liquid Crystals. *Phys. Rev. A* **1971**, *4*, 1238−1246.

(15) Yethiraj, A.; Sun, Z.; Dong, R. Y.; Burnell, E. E. NMR Measurement of Smectic Ordering and Nematic-Smectic-A Coupling in a Liquid Crystal. *Chem. Phys. Lett.* **2004**, *398*, 517−521.

(16) Yethiraj, A.; Burnell, E. E.; Dong, R. Y. The Smectic Potential in a Liquid Crystal with a Reentrant Nematic Phase: NMR of Solutes. *Chem. Phys. Lett.* **2007**, *441*, 245−249.

(17) Burnell, E. E.; Dong, R. Y.; Weber, A. C. J.; Yang, X.; Yethiraji, A. Separation of Nematic and Smectic-A Potential Effects on Solute Ordering in a Series of Binary 6OCB-8OCB Mixtures. *Can. J. Chem.* **2011**, *89*, 900−908.

(18) Cladis, P. E. New Liquid-Crystal Phase Diagram. *Phys. Rev. Lett.* **1975**, *35*, 48−51.

(19) Dong, R. Y. NMR Study of Alloys Exhibiting a Reentrant Nematic Phase. *J. Chem. Phys.* **1981**, *75*, 2621−2625.

(20) Sebastião, P. J.; Ribeiro, A. C.; Nguyen, H. T.; Noack, F. Molecular Dynamics in a Liquid Crystal with Reentrant Mesophases. *J. Phys. II* **1995**, *5*, 1707−1724.

(21) Weber, A. C. J.; Yang, X.; Dong, R. Y.; Meerts, W. L.; Burnell, E. E. Solute Order Parameters in Liquid Crystals from NMR Spectra Solved with Evolutionary Algorithms: Application of Double Maier−Saupe Kobayashi−McMillan Theory. *Chem. Phys. Lett.* **2009**, *476*, 116−119.

(22) Burnell, E. E.; de Lange, C. A.; Meerts, W. L. Novel Strategies for Solving Highly Complex NMR Spectra of Solutes in Liquid Crystals. In *Nuclear Magnetic Resonance Spectroscopy of Liquid Crystals*; Dong, R.Y., Ed.; World Scientific: Singapore, 2010; Chapter 1, p 1.

(23) Meerts, W. L.; de Lange, C. A.; Weber, A. C. J.; Burnell, E. E. *Encyclopedia of Magnetic Resonance, Analysis of Complex High-Resolution NMR Spectra by Sophisticated Evolutionary Strategies*; John Wiley & Sons Ltd.: New York, 2013; DOI: 10.1002/9780470034590.emrstm1309.

(24) Flory, P. J. *Statistical Mechanics of Chain Molecules*; Wiley-Interscience: New York, 1969.

(25) Maier, W.; Saupe, A. Eine Einfache Molekular-Statistische Theorie der Nematischen Kristallinflussigen Phase 0.1. *Z. Naturforsch. A* **1959**, *14*, 882−889.

(26) Maier, W.; Saupe, A. Eine Einfache Molekular-Statistische Theorie der Nematischen Kristallinflussigen Phase 0.2. *Z. Naturforsch. A* **1960**, *15*, 287−292.

(27) Burnell, E. E.; ter Beek, L. C.; Sun, Z. Mechanisms of Solute Orientational Order in Nematic Liquid Crystals. *J. Chem. Phys.* **2008**, *128*, 164901−164901−10.

(28) Burnell, E. E.; de Lange, C. A.; Barnhoorn, J. B. S.; Aben, I.; Levelt, P. F. Molecules with Large-Amplitude Torsional Motion Partially Oriented in a Nematic Liquid Crystal: Ethane and Isotopomers. *J. Phys. Chem. A* **2005**, *109*, 11027−11036.

(29) de Lange, C. A.; Meerts, W. L.; Weber, A. C. J.; Burnell, E. E. Scope and Limitations of Accurate Structure Determination of Solutes Dissolved in Liquid Crystals. *J. Phys. Chem. A* **2010**, *114*, 5878−5887.

(30) Yethiraj, A.; Weber, A. C. J.; Dong, R. Y.; Burnell, E. E. NMR Determination of Smectic Ordering of Probe Molecules. *J. Phys. Chem. B* **2007**, *111*, 1632−1639.
(31) Weber, A. C. J.; Yang, X.; Dong, R. Y.; Burnell, E. E. The Smectic Effect on Solute Order Parameters Rationalized by Double MaierSaupe KobayashiMcMillan Theory. *J. Chem. Phys.* **2010**, *132*, 034503−034503−8.
(32) Terzis, A. F.; Poon, C.-D.; Samulski, E. T.; Luz, Z.; Poupko, R.; Zimmermann, H.; Müller, K.; Toriumi, H.; Photinos, D. J. Shape-Dominated Ordering in Nematic Solvents. A Deuterium NMR Study of Cycloalkane Solutes. *J. Am. Chem. Soc.* **1996**, *118*, 2226−2234.